EPJ Web of Conferences **340**, 09015 (2025) https://doi.org/10.1051/epjconf/202534009015
Powders & Grains 2025

Shear flow of lubricant coated powder particles

Sayali V. Chaudhary[1,2] and *Ashish V.* Orpe[1,2,*]

[1]CSIR-National Chemical Laboratory, Pune 411008 India
[2]Academy of Scientific and Innovative Research (AcSIR), Ghaziabad 201002 India

Abstract. We have examined the lubrication between bulk powder particles flowing under gravity due to presence of a small content of tiny lubricant particles. The flow behavior of these particles is studied using discrete element method (DEM) simulations in an inclined chute system. The flow rate exhibits a non-monotonic dependence on the lubricant content, i.e. it initially increases with lubricant content while reaching a maximum followed by a decrease at larger lubricant contents. This is found to be in close qualitative agreement with the previous experimental study. While the increase in the flow rate is attributed to reduction in inter-particle friction due to presence of low friction lubricant particles at contact between bulk powder particles, the reduction in the flow rate is attributed to closed packing of a larger number of smaller sized lubricant particles leading to damping of momentum.

1 Introduction

Powder flowability plays a crucial role in many pharmaceutical processes, such as blending, die-filling and tablet compression and ejection [1]. Inter-particle friction can hinder smooth flow, affecting process efficiency and product quality. Lubrication is essential to mitigate these frictional effects, typically achieved by adding tiny quantities (weight ratio of $O[10^{-2}]$) of smaller, low friction powder particles. Magnesium stearate (MgSt) is the most commonly used lubricant in pharmaceutical applications [1]. These are plate-like particles which adhere to the surface of bulk powder particles, thereby modifying inter-particle interaction [1]. Although the impact of lubricant content on friction reduction and improved flowability is understood qualitatively and various studies have explored the factors influencing powder flowability [1–4], the underlying mechanism is not quite clear. In a recent experimental investigation [5] on gravity-driven flow of lubricant-coated bulk powder particles, it was shown that the bulk powder flow rate exhibits a non-monotonic dependence on lubricant content. Based on heuristic arguments and simple measurements of static angle of repose (essentially friction coefficient), it was postulated that the observed behavior was due to competing effects of reduced inter-particle friction and increased damping due to inter-particle collisions. We explore this behavior in detail by employing three dimensional discrete element method (DEM) simulations to elucidate the possible underlying mechanisms for inter-particle lubrication. The simulation methodology is discussed next followed by results and conclusion.

2 Simulation Methodology

The Discrete Element Method (DEM) simulations were carried out using LIGGGHTS (LAMMPS Improved for General, Granular and Granular Heat Transfer Simulations), to study the flow of lubricated powder flow systems. The simulation was carried out in a box (see fig. 1) of width $5d_p$, length $5d_p$ and height $7d_p$, where, d_p represents the diameter of the bulk powder particle. The x-axis represents flow direction, y-axis being transverse to the flow and z-axis representing the height. Periodic boundary conditions are maintained in $x-$ and $y-$ directions to prevent any boundary effects in these directions. The bottom surface is created from the particles of the same type and size as bulk powder particles, arranged in a simple cubic lattice to represent a rough boundary over which the particles flow, while the flow remains unbounded in z-direction, typical of a free surface flow. The bottom surface is maintained inclined at a predefined angle to the horizontal.

Both, bulk as well as lubricant powder particles are modeled as spheres, with bulk particles having 15% polydispersity. The bulk particles are maintained 10 times larger in size and 2.4 times heavier than the lubricant particles. The size ratio is so chosen to reduce the computation time while allowing for capturing relevant flow behavior qualitatively similar to the experiments [5]. The particles, both bulk as well as lubricant particles, are initially filled in the box upto an approximate height of $7d_p$.

The simulation employs Hertzian contact model for calculation of force between two contacting particles.The contact force is expressed in terms of normal (F_n) and tangential (F_t) components, each of which includes two terms given as

$$\boldsymbol{F_n} = \sqrt{\delta R^*}\,(k_n\delta \boldsymbol{n} - \gamma_n \boldsymbol{v}_n) \quad (1)$$

$$\boldsymbol{F_t} = -\sqrt{\delta R^*}\,(k_t\Delta \boldsymbol{s}_t + \gamma_t \boldsymbol{v}_t) \quad (2)$$

*e-mail: av.orpe@ncl.res.in

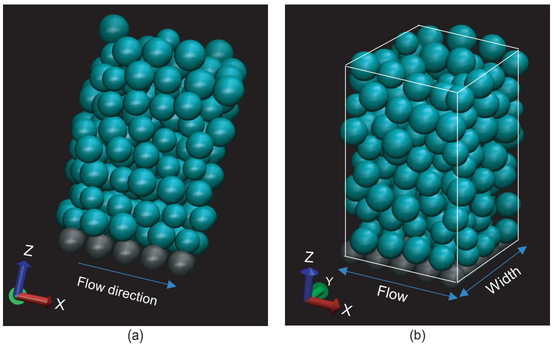

Figure 1. Simulation box (a) side view and (b) front view for modeling chute flow for an inclination angle of 24 degrees and $N_r = 0$.

where, $\boldsymbol{n}$ is the unit vector along the line connecting centers of two particles, δ denotes the normal overlap distance between two interacting particles, defined as the difference between the sum of their radii and the center-to-center distance at the point of contact, R^* is the effective radius of two interacting particles, $\boldsymbol{v}_t$ and $\boldsymbol{v}_n$ are, respectively, the tangential and normal components of particle velocities and $\Delta \boldsymbol{s}_t$ is the tangential displacement between two particles. Static friction is applied via the Coulomb yield criterion ($\boldsymbol{F_t} = \mu_s.\boldsymbol{F_t}$). Parameters are non-dimensionalized with bulk particle diameter $d_p = 1$, mass $m_p = 1$, and gravity $g = 1$. Hertzian elastic constants, k_n and k_t, are set to $O(10^6 m_\alpha g/d_\alpha)$, where m_α and d_α refers to the mass and diameter of either a bulk granular particle d_p or a lubricant particle d_l, depending on the interacting pair. Hertzian damping constants, γ_n and γ_t, are selected to obtain desired coefficient of restitution (e) shown for all cases in Table 1. Typically, the lubricant particles get attached to the surface of the bulk particles through a cohesive/adhesive force. To account for this interaction, the cohesion between lubricant and bulk particles is modeled using a simplified Johnson-Kendall-Roberts (SJKR) approach, adding a normal force dependent on contact area. A cohesion energy density of $C = 8 \times 10^4 m_\alpha g/d_\alpha^2$ maintains a stable overlap of approximately 0.5% of the particle radius. Simulations employ a natural time unit $\tau = \sqrt{d/g}$ with an integration time step of $\delta t = 10^{-5}$ to ensure temporal accuracy.

The mixture of bulk powder particles and pre-defined number of lubricant particles are filled in the box, maintained inclined at 24 degrees to the horizontal as in previous experimental study [5]. The lubricant particles adhere to the surface of the bulk powder particles due to cohesive interactions. Initially, the particles are poured in simulation box bounded by the side walls. The particles are filled approximately upto a height of $7d_p$ followed by removal of bounding walls to initiate the flow as in experiments. As the simulation progresses in time the flow restructures and adjusts the flowing thickness while re-distributing the lubricant particles across bulk particles. The simulations are continued until the system reaches steady state, defined as the flow wherein the total kinetic energy over all particles remains constant within 1 % of the mean value. All the further analysis is carried out in the steady state flow regime obtained over a time duration equivalent to mean distance traveled by the flow of at least $2000d_p$. The lubricant concentration is specified in terms of number ratio (N_r) of lubricant to bulk particles. For each value of N_r, the average bulk (p) particle velocity profile was obtained in the flowing layer by averaging over 1000-time instants spaced uniformly within the steady state regime. The flow depth (thickness) profile obtained from these velocity profile was then multiplied by the flow cross-section, defined as width × thickness (or height), to obtain the mean flow rate ($\langle Q_p \rangle$) of bulk particles in the flowing layer.

Table 1. Values of coefficient of friction and restitution for different pairs of particles used in simulations

Parameters	Values
Bulk inter-particle friction coefficient (μ_{pp})	0.3
Bulk-bed friction coefficient (μ_{pb})	0.2
Lubricant-lubricant friction coefficient (μ_{ll})	0.01
Lubricant-bulk friction coefficient (μ_{lp})	0.1
Lubricant-bed friction coefficient (μ_{lb})	0.1
Coefficient of Restitution (e_{pp}, e_{pb})	0.7
Coefficient of Restitution (e_{ll})	0.051
Coefficient of restitution (e_{lp}, e_{lb})	0.3

Given two particle types in the system, substantial tuning of the interaction parameters is needed to get realistic flow representation. The values for inter-particle (pp) and particle-rough bed (pb) restitution coefficient for bulk particles, e_{pp} and e_{pb}, respectively were obtained from literature [6, 7]. The values for inter-particle friction coefficient (μ_{pp}) and particle-rough bed friction coefficient (μ_{pb}) for the bulk particles were adjusted to match the velocity profiles from simulations to that in experiments with bulk particle flow [5]. Considering their lower friction [8] and highly dissipative nature [9], the values of inter-particle friction (μ_{ll}) and coefficient of restitution (e_{ll}) for the lubricant (l) particles were assumed to be 0.01 and 0.051, respectively. The rest of the parameters, lubricant-bulk particle (μ_{lp}) and lubricant-rough bed (μ_{lb}) friction coefficients and lubricant-bulk particle (e_{lp}) and lubricant-rough bed (e_{lb}) co-efficient of restitution were assumed, as these values are not readily available from literature. All interaction parameter values are listed in table 1.

3 Results and Discussion

The variation of normalised, mean flow rate ($\langle Q_p \rangle / \langle Q_{p0} \rangle$) of bulk particles with the number ratio N_r is shown in fig. 2. Here, $\langle Q_{p0} \rangle$ represents the base case flow rate, i.e. flow of bulk particles in absence of lubricant particles. A non-monotonic trend is evident, wherein the flow rate increases with increase in N_r, reaches a maximum around $N_r = 300$ and then decreases for further increase in N_r. While this behavior is qualitatively similar to that observed in experiments previously [5], the maximum increase in flow rate in simulations is about 7 times that of the base case compared to the experiments which show a maximum increase around 1.3−1.5 times the base case. We, next, discuss the origins of the observed non-monotonic behavior and the quantitative differences with experimental results.

Figure 3 shows the steady state simulation snapshot for four different values of N_r. Large blue spheres are the bulk particles while small yellow spheres are lubricant particles. The flowing layer appears quite dense and compact in absence of lubricant particles. For $N_r = 100$, the lubricant particles are well dispersed within the bulk particles. Many of them coat the large particles, while remaining randomly connected to other lubricant particles. Note that the lubricant particles adhere to bulk particles due to cohesive forces between them and remain dispersed uniformly in the system, otherwise for a size difference of 10, segregation can be expected. The coating of lubricant particles over larger particles reduces the contact between frictional large particles and increases between lower frictional lubricant particles, thereby quickening the flow rate. We believe that fast flow results in increased collision leading to flow expansion. This behavior, qualitatively resembles that observed in previous experiments [5].

For a further increase in lubricant (upto $N_r = 300$), the flow becomes substantially dilated and expands upto nearly $2-3$ times the flow thickness in the base case. Such an expansion is not observed in experiments and is only exclusive to simulations. The coating of bulk particles by the lubricant is nearly complete in this case, leading to much reduced friction and increased flow rate. Such uniform coating is not observed in experiments [10]. Further, the lubricant particles in simulations are relatively larger, spherical in size thereby allowing them to flow independently leading to excessive collisional flow, hence more expansion and much faster flow. The plate-like particles used in experiments, which are also smaller in size do not flow independently thereby limiting the flow expansion. For an even further increase in $N_r = 600$, the flow is now dominated by much closely packed lubricant particles. We believe this leads to larger damping resulting in denser, more compact flowing layer and lower flow rate. It is expected that an even further increase in the lubricant content will slow down the flow even further and possibly even lower than the base case, thereby nullifying the utility of lubricant particles as also observed in experiments [5].

We also carried out simulations for only bulk particles in a box with larger base ($20d_P \times 20d_p$ as in experiments), while keeping the flow height and chute inclination angle constant to determine the size effects. The flow rate was about 20% smaller in larger box indicating the magnitude of the size effects. However, this difference is quite small compared to the flow rate differences (about $3-4$ times) observed between experiments and simulations, thereby indicating that the predominant reason for the discrepancy was due to spherical shaped and larger size lubricant particle used in simulations compared to smaller sized and plate-like in experiments as discussed above.

To understand the above discussed qualitative behavior further and to support our arguments, we analysed several images similar to those shown in fig. 3 to obtain some quantitative information. Essentially, the observed flow behavior is due to interaction between different particles

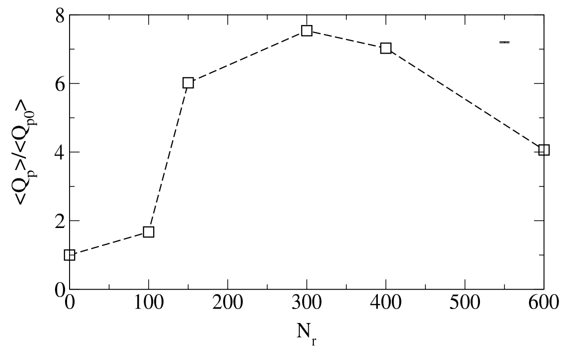

Figure 2. Variation of normalised, mean flow rate ($\langle Q_p\rangle/\langle Q_{p0}\rangle$) with lubricant content (N_r). Representative error bar is presented in the top-right corner since actual error bars are smaller than symbol size.

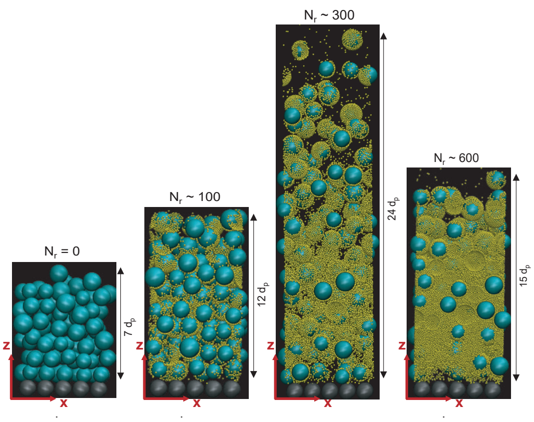

Figure 3. Flow layer and particle positions in $x-z$ plane at one particular time within the steady state regime for different values of N_r. Blue spheres represent bulk (b) particles while yellow spheres represent lubricant (l) particles.

on contact. We considered 1000 different time instants spread uniformly over the steady state duration and calculated the average of all inter-particle binary contacts obtained for each of these time instants. Three types of contacts are identified, viz. bulk-bulk (p-p), bulk-lubricant (p-l) and lubricant-lubricant (l-l) with the average number of contacts, respectively, defined as $\langle n_{pp}\rangle$, $\langle n_{pl}\rangle$ and $\langle n_{ll}\rangle$. A contact between two particles is defined whenever the distance between the centers of two particles is lesser than the sum of the radius of both particles (i.e. overlapping particles).

Figure 4 shows the variation of average number of contacts per time instant with lubricant content. The y-axis on the left side represents $p-p$ contacts while that on the right side represents $p-l$ and $l-l$ contacts. The value of $\langle n_{pp}\rangle$ decreases monotonically while that of $\langle n_{pl}\rangle$ and $\langle n_{ll}\rangle$ increase monotonically as would be expected on increasing lubricant content. The decreasing and increasing trend, respectively, for $\langle n_{pp}\rangle$ and $\langle n_{pl}\rangle$ represent progressively increasing coating of lubricant particles thereby reducing contacts between bulk particles. The contacts between bulk particles progressively occurs predominantly

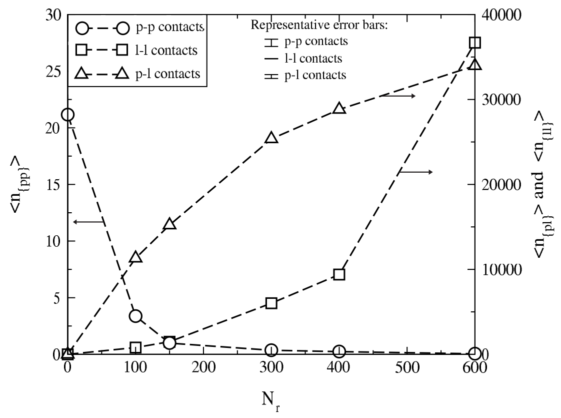

Figure 4. Variation of average number of inter-particle binary contacts per time instant with the particle number ratio (N_r). Representative error bars are presented in the top-right corner since actual error bars are smaller than symbol size.

through intermediate, coated lubricant particles, thereby reducing overall friction in the system and higher flow rate. On reaching $N_r = 300$, the value of $\langle n_{pp} \rangle$ is almost negligible compared to its value at $N_r = 0$. This indicates substantial coating of the bulk particle surface by lubricant particles as also evidenced by substantial increase in the value of $\langle n_{pl} \rangle$, thereby nearly eliminating bulk particle friction and highest flow rate value. For further increase in N_r, the value of $\langle n_{pp} \rangle$ continues to decrease, but that of $\langle n_{pl} \rangle$ increases at a slower rate. This is due to progressively lesser area of bulk particle surface available for coating. This leads to increasing number of non-coating, freely dispersed lubricant particles, as evidenced by rapid increase in the value of $\langle n_{ll} \rangle$. This rapid addition of lubricant particles results in overall closed packing of particles, more dissipation which overwhelms the effect of lubrication, hence reduced flow rate. At very high values of N_r (not shown), the value of n_{pl} can be expected to reach constant value (complete coverage) accompanied by $n_{pp} = 0$ (no bulk particle contact) and enormous increase in the value of n_{ll} (substantial presence of flowing lubricant particles). In that case, the flow rate can be expected to be lower than even the base case, essentially nullifying the lubrication and pointing towards need for optimality of lubricant concentration for best possible flow behavior [5, 10].

4 Conclusion

We have studied the flow behavior of powder lubricant coated powder particles in an inclined chute system for a fixed inclination angle, fixed size of bulk and lubricant particles and increasing lubricant content using DEM simulations. The flow rate of bulk particles exhibits a non-monotonic dependence on the lubricant content in agreement with previous experimental measurements [5]. The increased lubrication due to increased coating of the bulk particles by the lower friction lubricant particles is explained using visualisation and captured quantitatively through inter-particle contacts. The same calculated variables are also used to explain the effective decrease in lubrication at higher lubricant content.

It is interesting to note that the lubricant particles modeled as spheres are able to capture the qualitative experimental behavior obtained using plate-like particles. The reason, perhaps, being that the friction is an inter-particle contact phenomena and the contact, whether due to a sphere or a plate-like, should not affect the qualitative behavior. However, the other effect of using spherical lubricant particles is the excess increase in the flow rate compared to the base case than that observed in experiments. This is because of independent flow of spherical lubricant particles in the systems not possible for the plate-like particles. Nevertheless, the simulations have allowed for suitable understanding and explaining the non-monotonic dependence flow behavior on the lubricant content. It would be interesting to understand the effect of bulk particle shape on the overall behavior which is relegated to a future study.

Acknowledgements

The authors are grateful to Dr. Pankaj Doshi for several fruitful discussions and insightful suggestions. The authors gratefully acknowledge the financial support from Science & Engineering Research Board, India (Grant No. CRG/2019/000423) and the "CSIR centralized HPC, AI & ML Platform (CHAMP) facility" provided by CSIR-4PI, Bengaluru, “PARAM Brahma Facility” at the IISER, Pune and the“Einstein cluster facility” at CSIR-NCL Pune.

References

[1] G. Morin, L. Briens, AAPS PharmSciTech **14**, 1158 (2013).
[2] F. Danish, E. Parrott, Journal of Pharmaceutical Sciences **60**, 752 (1971).
[3] Y. Wang, J.G. Osorio, T. Li, F.J. Muzzio, Powder Technology **322**, 332 (2017).
[4] M. Yoshida, R. Takatsuki, G. Sakamoto, J. Oshitani, K. Gotoh, Advanced Powder Technology **27**, 2084 (2016).
[5] R.S. Ghodake, P. Doshi, A.V. Orpe, Powder Technology **409**, 117809 (2022).
[6] L.E. Silbert, D. Ertaş, G.S. Grest, T.C. Halsey, D. Levine, S.J. Plimpton, Physical Review E **64**, 051302 (2001).
[7] S. Zhang, G. Yang, P. Lin, L. Chen, L. Yang, The European Physical Journal E **42**, 40 (2019).
[8] T. Miller, P. York, Powder Technology **44**, 219 (1985).
[9] E. Serris, A. Sato, A. Chamayou, L. Galet, M. Baron, P. Grosseau, G. Thomas, in *Powders and Grains* (2013), pp. 779–782
[10] R.S. Ghodake, A.V. Orpe, manuscript submitted for publication